# Benchmark Evaluation of Light Charged Particle Production

Franz X. Gallmeier
Oak Ridge National Laboratory

January 20, 2010

## Importance

In the past, the prediction of charged particle emission other than protons has been second priority for spallation models. Energy deposition in materials in accelerator applications is usually dominated by continuous slowing down of the incident particles, and shielding is dominated by the high-energy tail of neutron emission. With accelerator powers approaching and exceeding the megawatt level as for the new generation spallation neutron sources and next generation rare isotope accelerator and irradiation facilities, hydrogen and helium build up in materials has an impact on material damage causing swelling and has renewed the effort of a proper description. Also the generation of spallation products beyond the sum of masses of the target and projectile nuclei is driven by reactions initiated by secondary light charged particles. And last but not least, the residual nuclei production can only be predicted correctly, when all emission channels including the charged particles are described adequately by the codes.

## Previous Light Charged Particle Benchmarking efforts

In the years 1992/93 the "International Code Comparison for Intermediate Nuclear Data" was conducted with the aim "to determine the predictive power of current nuclear reaction models and codes in the intermediate energy range." The report abstract clearly states the extension of the effort:

> "Emphasis has been placed on thin target double differential cross sections, for which $^{90}$Zr and $^{208}$Pb target nuclei were selected. Experimental double differential cross section data are compared with calculated results at incident proton energies of 25, 45, 80, 160, 256 and 800 MeV for (p, xn) reactions, and at incident energies of 80 and 160 MeV for $^{90}$Zr (p, xp) reactions. Calculated (p, xp) double differential spectra are presented at 25, 45, 256, 800 and 1600 MeV, and (p, xn) double differential cross sections are presented at 1600 MeV; however, no comparisons with experimental data are made for these cases."

This effort exercised INC+deexcitation codes (including one QMD code) and precompound nuclear reaction models, the later being limited to projectile energies below 200 MeV.
Comparison of charged particle emission other than protons was not considered. There is no overlap between the present and former benchmark; Zirconium is not considered as a

target in the present benchmark, the energies of 80 and 160 MeV of the former benchmark effort are matched at best by 62-63 MeV protons on natural Fe and 175 MeV protons on natural Ni of the present benchmark. A measure of the predictive power of the codes from1992 is given by the later addition of the MCNPX-Bertini-Dresner contribution, which uses nuclear models that are essentially equivalent to the LAHET contributions from year 1992. Proton double-differential cross sections of the previous benchmark are shown in Figs. 1-4, where the experimental data are described by the lined up points and the LAHET predictions given by the symbol ×. Half of the calculated points are contributed by precompound models, which are matching the experimental data typically better than INC+deexcitation models. This gives the impression of a general good agreement between models and experiment, which for the INC codes is not true.

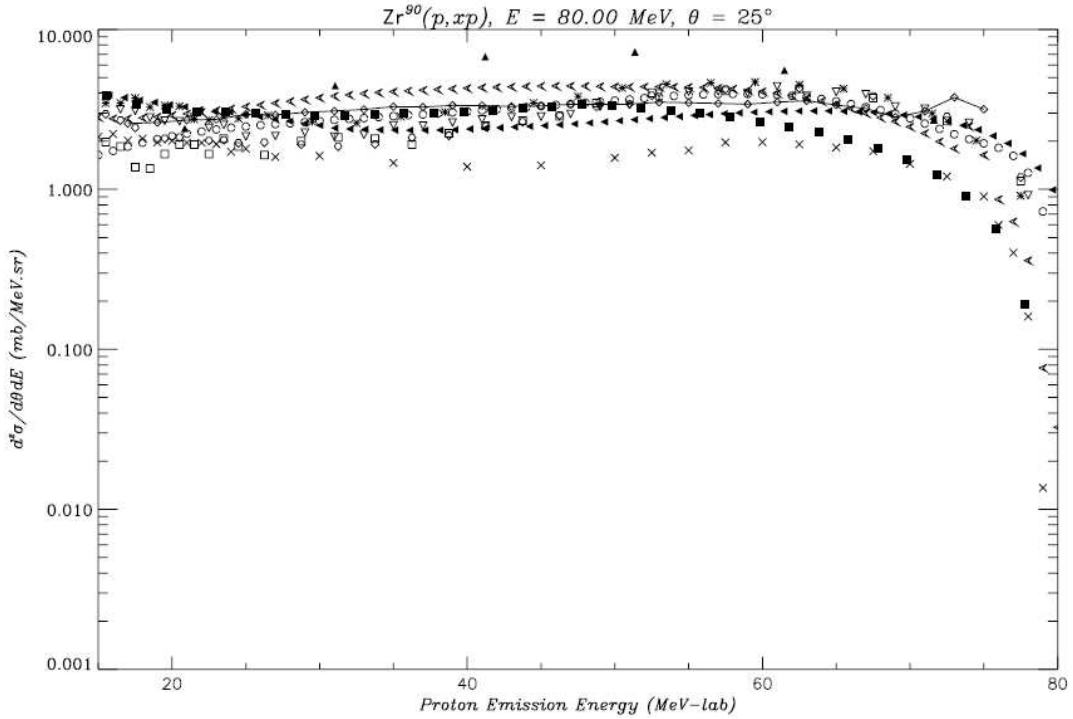


Fig.1: Results from previous benchmark effort (80 MeV protons on Zr-90; protons in 25 degree): points with connected lines show experimental data, symbol × mark LAHET results.

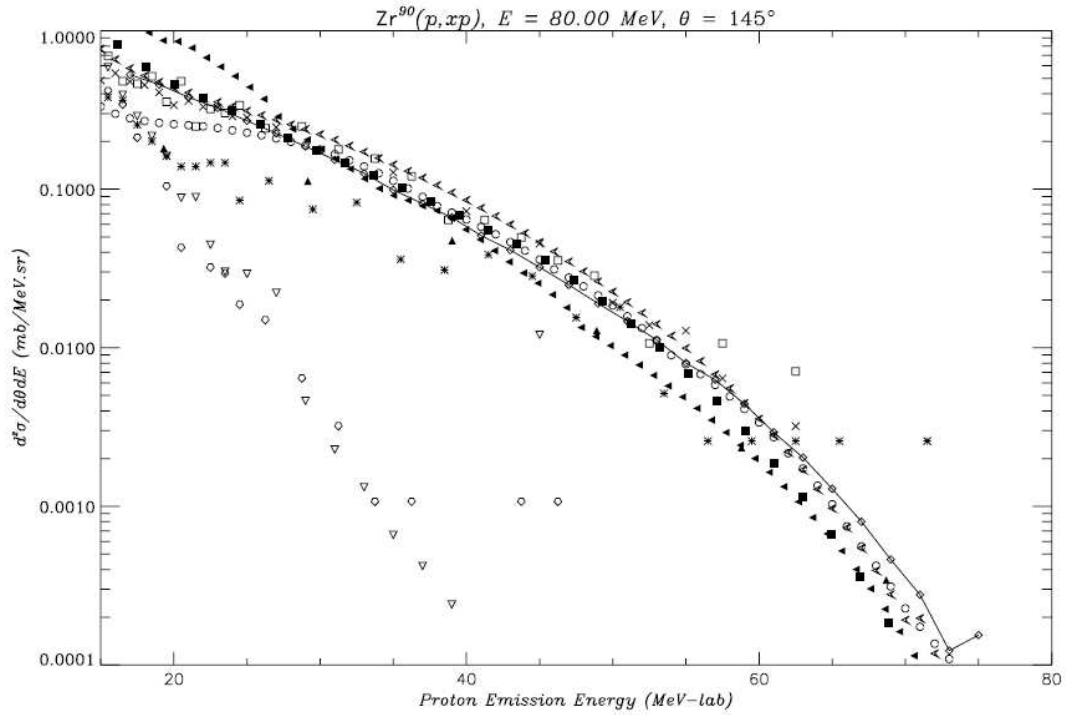


Fig.2: Results from previous benchmark effort (80 MeV protons on Zr-90; protons in 145 degree): points with connected lines show experimental data, symbol × mark LAHET results.

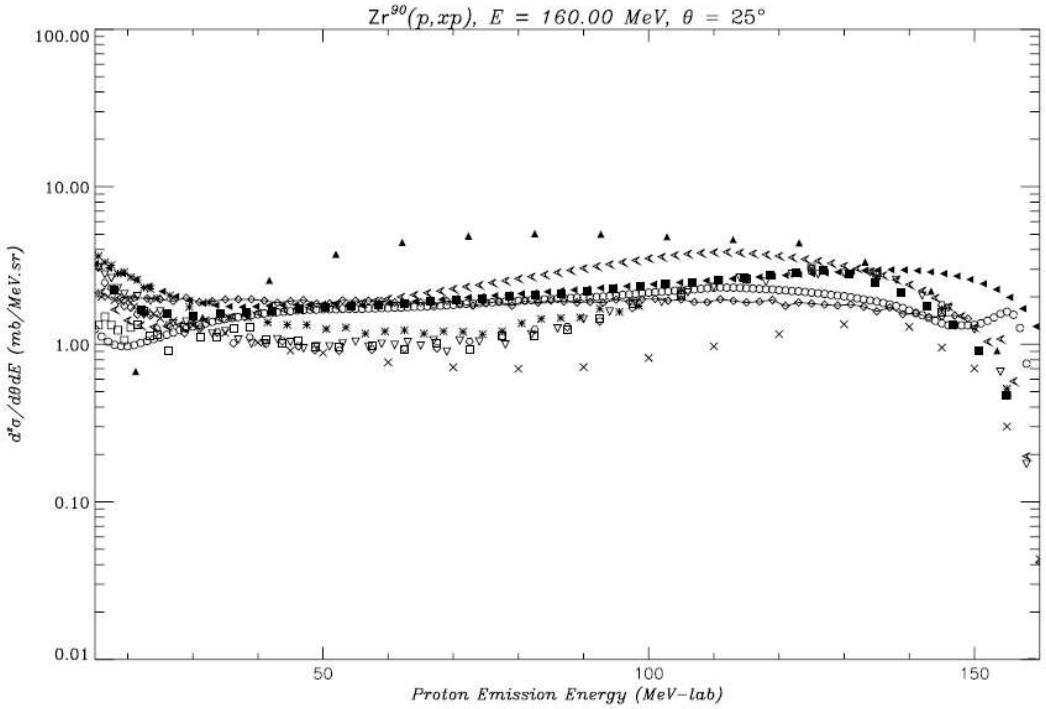


Fig.3: Results from previous benchmark effort (160 MeV protons on Zr-90; protons in 25 degree): points with connected lines show experimental data, symbol × mark LAHET results.

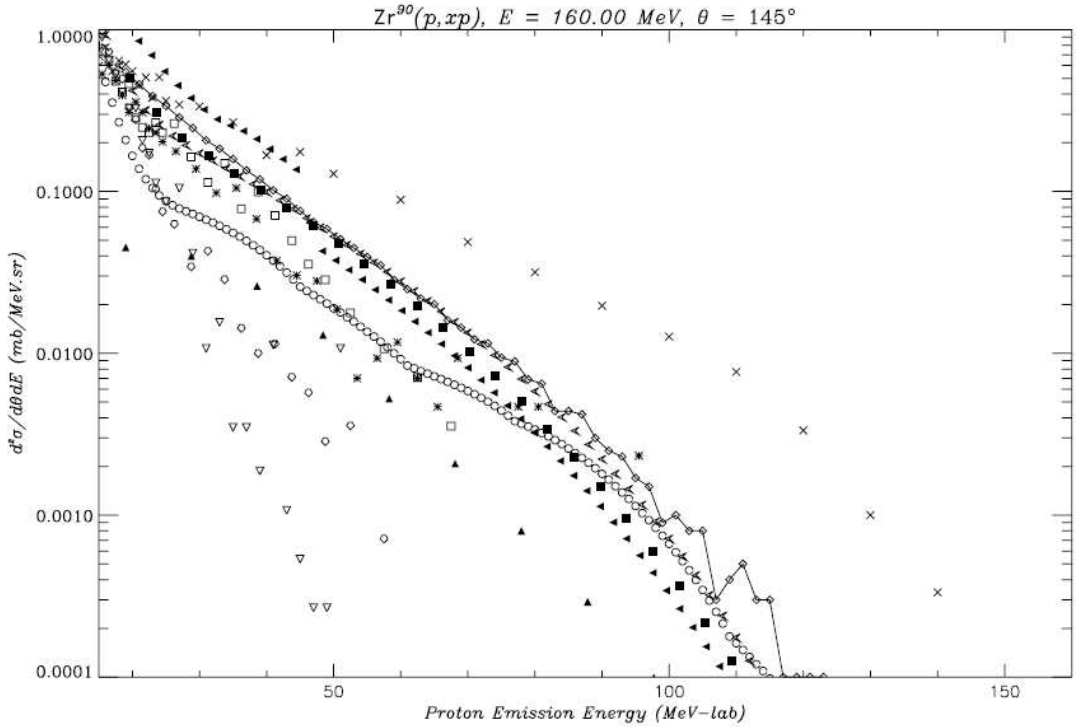

Fig.4: Results from previous benchmark effort (160 MeV protons on Zr-90; protons in 145 degree): points with connected lines show experimental data, symbol × mark LAHET results.

**Experimental data**

The initiators of the present Spallation Benchmarking Effort have selected experimental data of production cross sections of light charged particles differentiated in energy and angle as listed in Table 1. With regard to the time of the previous benchmark effort, a number of experiments of charged particle emission on thin targets have been conducted and contributed a wealth of double-differential cross sections to the EXFOR data base mainly by experiments completed in Germany at the COSY facility. The target materials selected here cover mainly medium to high mass elements excluding actinides. Benchmarking low mass target element spallation was deferred to a later time. Except for the experiment of 542 MeV neutrons on Bi, all experiments were conducted with protons as the projectile. The incident energies span from 60 to 2500 MeV and are covering well the range of validity of spallation models. The selection of data did not consider medium mass elements at beam energies of 800 MeV and above although published data exists.

The selected experimental data covers emission of protons, deuterons, tritons, $^{3}$He, and alpha particles. Some of the experiments cover only a subset of the emitted particles. The emission of light charged particles was considered at various emission angles ranging from 11 to 164 degrees. Data for emission at extreme forward and backward directions with regard to the beam direction are not available.

Table 1: Listing of experimental data selected for the light charged particle emission benchmark.

| Beam | Target | Beam Energy [MeV] | Emitted particles | Emission angles [deg] | Emission energies [MeV] | Reference |
|---|---|---|---|---|---|---|
| n | Bi | 542 | p, d, t | 54 -164 | 20-500 | J. Franz et al., Nucl. Phys. A 510 (1990) 774 |
| p | Al | 160 | α | 20-140 | 20-160 | A. Cowley et al., Phys. Rev. C 54 (1996) 778 |
| p | Fe | 62 | p, d, t, $^3$He, α | 20-135 | 5-62 | F.E. Bertrand and R.W. Pelle, Phys. Rev. C 8 (1973) 1045 |
| p | Ni | 175 | p, d, t, $^3$He, α<br>p | 16-100<br>15-120 | 2-175<br>20-175 | F. Goldenbaum et al., (unpublished)<br>S.V. Förtsch et al., Phys. Rev. C 43 (1991) 691 |
| p | Ta | 1200 | p, d, t, $^3$He, α | 30-150 | 2-100 | C.-M. Herbach et al., Nucl. Phys. A 765 (2006) 426 |
| p | Au | 160 | α | 20-140 | 20-160 | A. Cowley et al., Phys. Rev. C 54 (1996) 778 |
| p | Au | 1200 | p, d, t, $^3$He, α | 16-100 | 2-250 | A. Budzanowski et al., Phys. Rev. C 78 (2008) 024603 |
| p | Au | 2500 | p, d, t, $^3$He, α | 30-150<br>16-100 | 2-150<br>2-150 | A. Letourneau et al., Nucl. Phys. A 712 (2002) 133<br>A. Bubak et al., Phys. Rev. C 76 (2007) 014618 |
| p | Pb | 63 | p, d, t, $^3$He, α | 25-155 | 5-60 | A. Guertin et al., Eur. Phys. J. A 23 (2005) 49 |
| p | Pb208 | 800 | p | 11-30<br>5-30 | 200-800<br>50-800 | R. Chrien et al., Phys. Rev. C 21 (1980) 1014<br>J.A. McGill et al., Phys. Rev. C 29 (1984) 204 |
| p | Bi | 62 | p, d, t, $^3$He, α | 15-160 | 5-60 | F.E. Bertrand and R.W. Pelle, Phys. Rev. C 8 (1973) 1045 |

Most of the experimental data cover particle emission energies of 10-150 MeV. Only four experiments - Franz, Budzanowski, Chrien and McGill - performed measurements at higher energies, but all of them only for protons except for Franz ,et al, also checking into deuterons and tritons. For future benchmarking efforts, experimental data extending into the high energy tail may be desirable.

With the groups of Goldenbaum and Frötsch investigating 175 MeV protons on nickel, and the groups of Chrien and McGill studying 800 MeV protons on lead, we have two cases of two independent groups providing redundant experimental data for proton emission. The comparison of the double-differential cross sections in these cases shown in Figures 5 and 6 confirm that the experimental data are generally consistent but also indicate local deviations mostly within the experimental error. Considering that Goldenbaum used the Frötsch data for normalization, the absolute agreement is not really surprising, but the agreement of the spectral shapes is.

In addition the groups of Letourneau and Bubak were independently measuring proton, deuteron, triton, He-3 and alpha double differential production cross sections that are compared in five plots of Figure 7. Again most of the data sets agree well within the errorbars with outliers of upto a factor of 2 at 70 and 100 degree proton emission.

These comparisons increase our confidence in the quality of the experimental data. We are confident that the provided data is a good basis - after all benchmarking is as good as the provided experimental data.

The available experimental data are not complete enough to allow an estimate of secondary particle multiplicities, which would be an interesting quantity to compare. Excitation functions of He-3 and He-4 discussed in another chaper of the benchmark evaluation, give some insight .

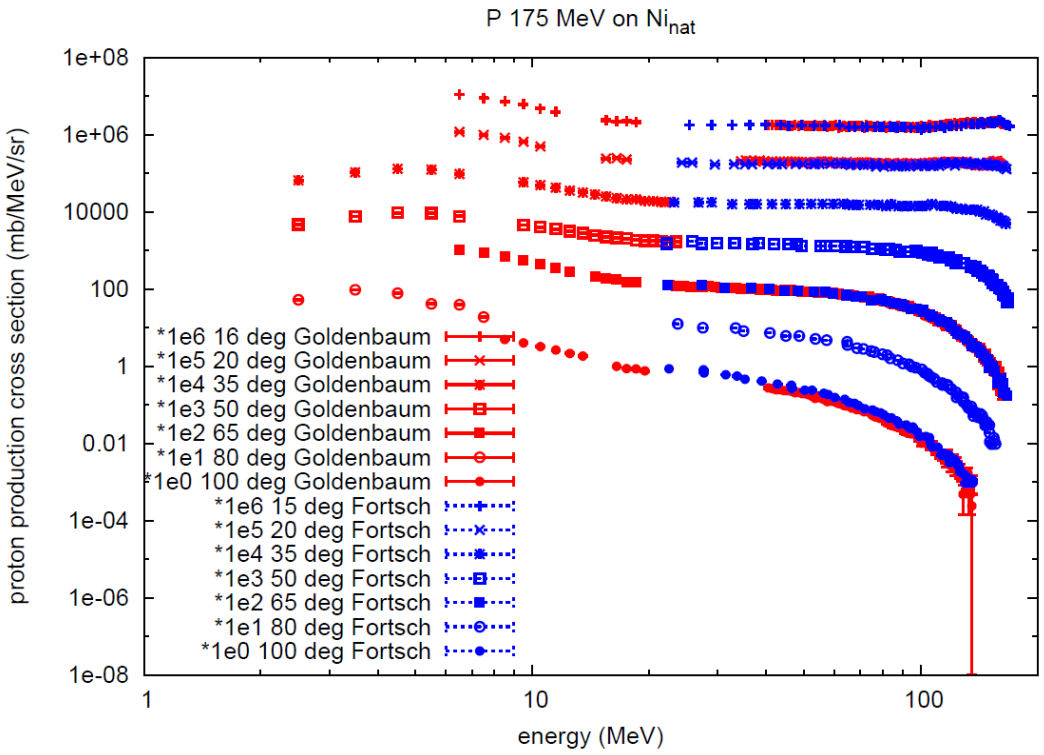


Figure 5: Comparison of double-differential proton production cross sections measured for 175 MeV protons on natural nickel by Goldenbaum et al and Frötsch et al.

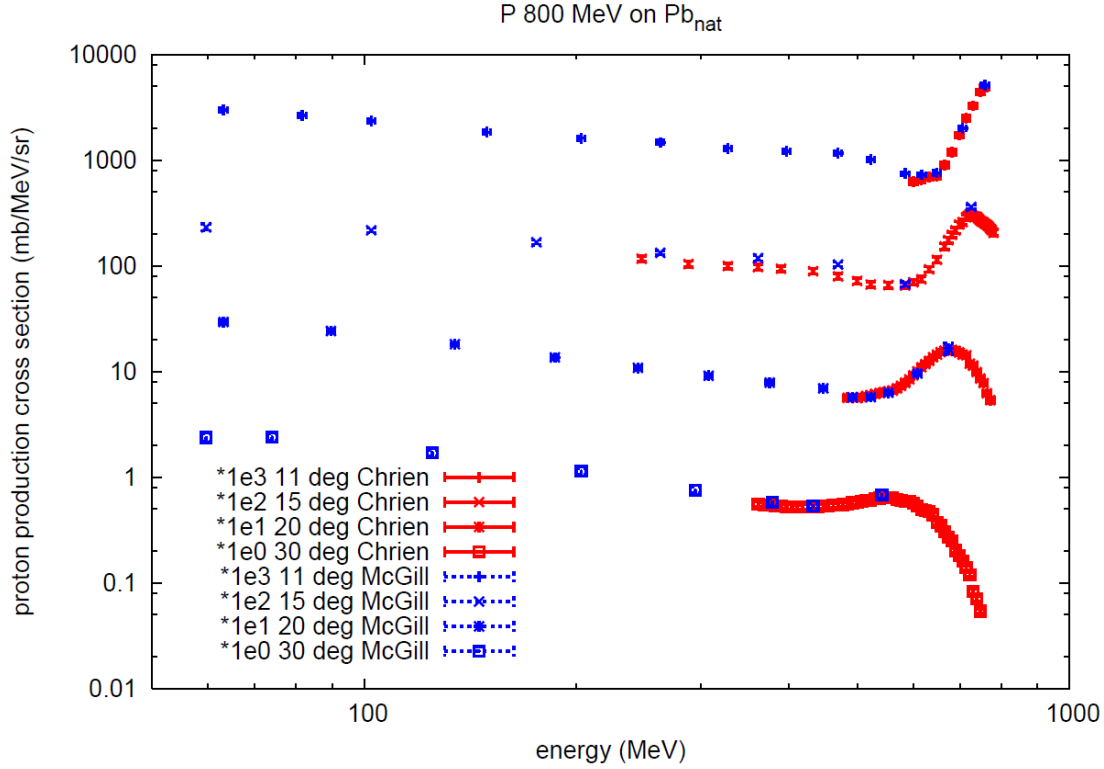


Figure 6: Comparison of double-differential proton production cross sections measured for 800 MeV protons on natural lead by Chrien et al and McGill et al.

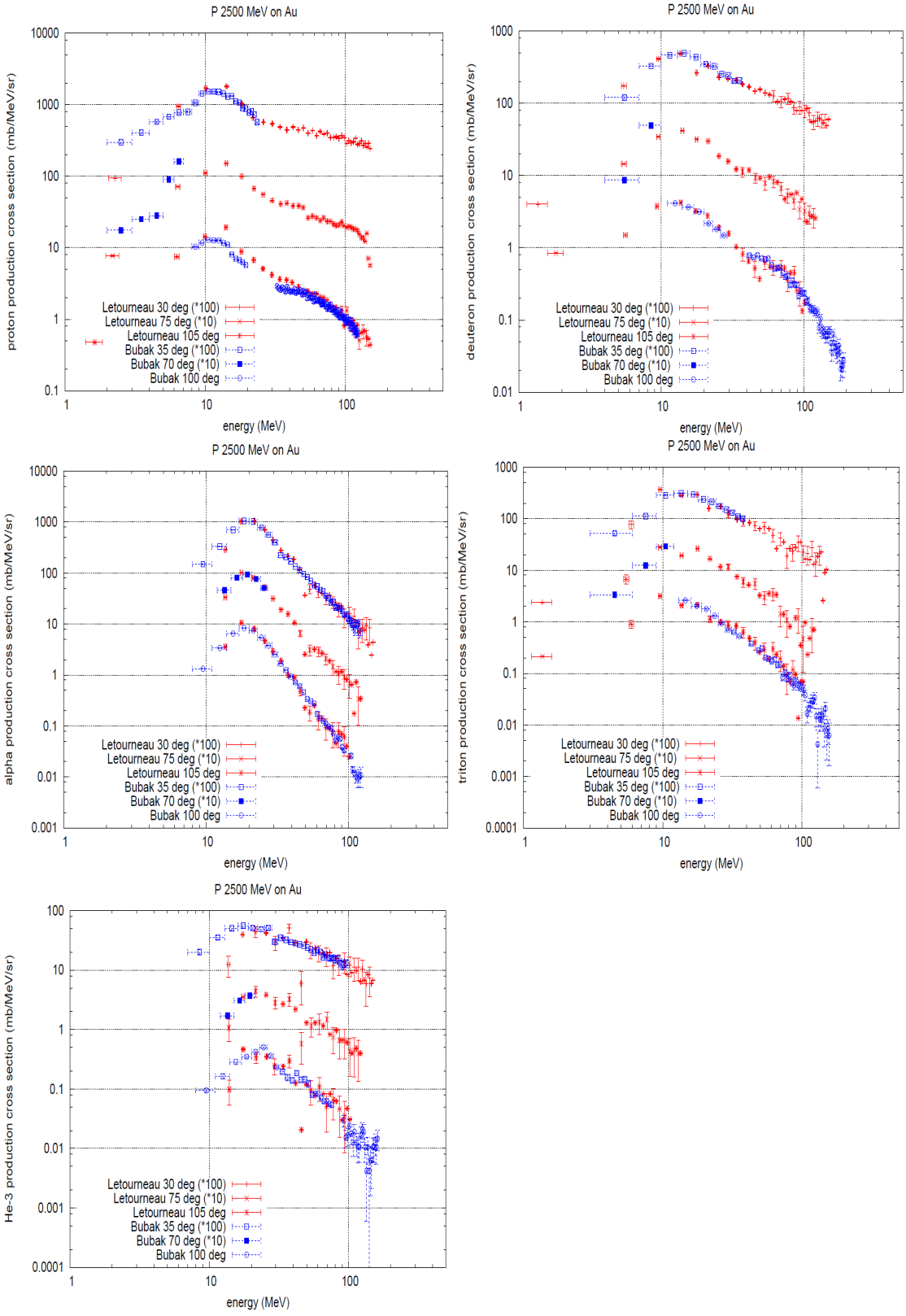


Figure 7: Comparing proton, deuteron, triton, He-3 and alpha double differential production cross sections from Letourneau, et al, and Bubak, et al for 2500 MeV protons on gold

**Contributing Models**

Results from seventeen models and codes were submitted to the benchmark. The list of participating models (in alphabetic order) and the abbreviations used throughout this report are given in Table 2. The contributing codes describe the reaction outcome by a intra-nuclear cascade or a QMD phase followed by a deexcitation phase. In some of the models a pre-equilibrium emission phase follows the INC phase. The naming convention is not conclusive: while the first part name fragments INCL4.5, ISABEL, indicate INC code phases, Geant4, MCNPX and PHITS indicate transport codes using the models following in the second part of the naming. The codes starting with Cascade and CEM describe monolithic code systems that have INC, preequilibrium and equilibrium deexcitation parts integrated.

Table 2: Nuclear modeling codes contributing to the light charged particle emission benchmark.

| **Model** | **Abreviation** | **Contributors** |
|---|---|---|
| Cascade04 | cascade04 | H. Kumawat |
| Cascade-ASF | Cascadeasf | A. Konobeyev |
| CEM0302 | cem0302 | S. Mashnik |
| CEM0303 | cem0303 | A. Gudima |
| Geant4-Bertini | g4bert | D. Wright |
| Geant4-BIC | g4bic | D. Wright |
| INCL4.5-ABLA07 | incl45-abla07 | J. Cugnon/ A. Boudard/ A. Kelic/ V. Ricciardi/ D. Mancusi |
| INCL4.5-Gemini | incl45-gemini++ | J. Cugnon/ A. Boudard/ R. Charity / D. Mancusi |
| INCL4.5-SMM | incl45-smm | J. Cugnon/ A. Boudard/ A. Botvina/ D. Mancusi |
| Isabel-ABLA07 | isabel-abla07 | Y.Yariv / A. Kelic / V. Ricciardi / D. Mancusi |
| Isabel-Gemini | isabel-gemini | Y.Yariv / R. Charity / D. Mancusi |
| Isabel-SMM | isabel-smm | Y.Yariv / A. Botvina / D. Mancusi |
| MCNPX_Bertini-Dresner | mcnpx-bert | F. Gallmeier/ W. Lu |
| PHITS-Bertini | phits-bertini | N. Matsuda |
| PHITS-jam | phits-jam | N. Matsuda |
| PHITS-JQMD | phits-jqmd | N. Matsuda |

**Preliminary Evaluation**

The IAEA website http://nds121.iaea.org/alberto/mediawiki-1.6.10/index.php/Benchmark:CalculRes provides plots of energy versus double-differential cross sections for all angles of the selected benchmark experiments. In addition a series of different figures-of-merit (FOM) based on deviations between experimental and calculated data is offered. The FOMs try to compress the wealth of data into easier to view and easier to interpret quantities. Each of the FOMs has its own characteristics and bias such that the set of FOMs does not give a coherent picture. They are not further discussed other than stating that the reviewer's rating scheme has similarities to the metric scoring the number of points into an experimental-value-centered acceptance band.

The nature of the benchmark results of light charged particles with large deviations between codes and experimental data leaned to an eye-guided rating scheme that allows for a coarse but quick screening of the results. For this reason, a simplified rating scheme was established.

**Rating Scheme**

The rating scheme is point based. A code earns points for the level of deviation achieved for each set of angular data of an experimental data set. The acceptance bands for the established four level scheme is given in Table 3. The energy ranges 0-150 MeV and above 150 MeV are rated separately if experimental data are present in both energy bands; otherwise only the energy band with experimental points is rated. If a code does not provide data for the range of the experimental data, it is considered to be deficient and does not earn any points.

Table 3: Rating scheme.

| Acceptance band [val/x ; val*x] | Earned points |
|---|---|
| x=5 | 1 |
| x=3 | 2 |
| x=2 | 3 |
| x=1.4 | 4 |

From the sum of each rating, an average rating for each experimental data set was calculated for each code and graphically presented in a histogram chart.

After completing a good part of the evaluation, the reviewer wished to have considered three energy ranges: 0-20 MeV, 20-150 MeV, and above 150 MeV. This detailing may be completed later in a later more rigorous rating approach.

## Selection of Data for 1st Stage Evaluation

Considering the wealth of calculated data, a subset of about half of the experimental data was chosen for the preliminary evaluation of the emission of light charged particles to be able to finish the evaluation within reasonable time. The selection was guided by

- considering data for all light charged particles,
- selecting from all different target materials,
- covering the whole range of beam energies and secondary particle energies,
- selecting data with as wide as possible angular range.

Table 4: Selection of experimental data for 1st Stage of benchmark evaluation

| Beam | Target | Beam Energy [MeV] | Emitted particles | Emission angles [deg] | Emission energies [MeV] |
|---|---|---|---|---|---|
| n | Bi | 542 | p, d, t | 54 -164 | 20-500 |
| p | Fe | 62 | p, d, t, $^3$He, α | 20-135 | 5-62 |
| p | Ni | 175 | p, d, t, $^3$He, α | 16-100 | 2-175 |
| p | Ta | 1200 | p, d, t, $^3$He, α | 30-150 | 2-100 |
| p | Au | 2500 | p, d, t, $^3$He, α | 16-100 | 2-150 |
| p | Pb208 | 800 | p | 5-30 | 50-800 |

## General Benchmark Findings

The rating results for each benchmark data set and each light charged particle are given in Figs A1-6 in the Appendix.

Calculated data for the CASCAD04 code were not available for 175 MeV protons on $Ni_{nat.}$ Almost all of the PHITS-JQMD contributed data have very large statistical errors resulting in poor ratings. With lower statistical errors this code very likely would have fared better.

The results indicate that no particular code is able to predict all the considered experimental data for all light charged particles within a factor of 3 (rating=2) or better. The worst case of prediction was He-3 emission into 20 degrees in the data set 62 MeV protons on Fe-56 as shown in Fig. 7(a) (discussed in more depth later), where no code earned a point. The best case prediction was 65 degree proton emission for 175 MeV protons on natural nickel (see Figs. 7(b)), where every code earned 3 or 4 points.

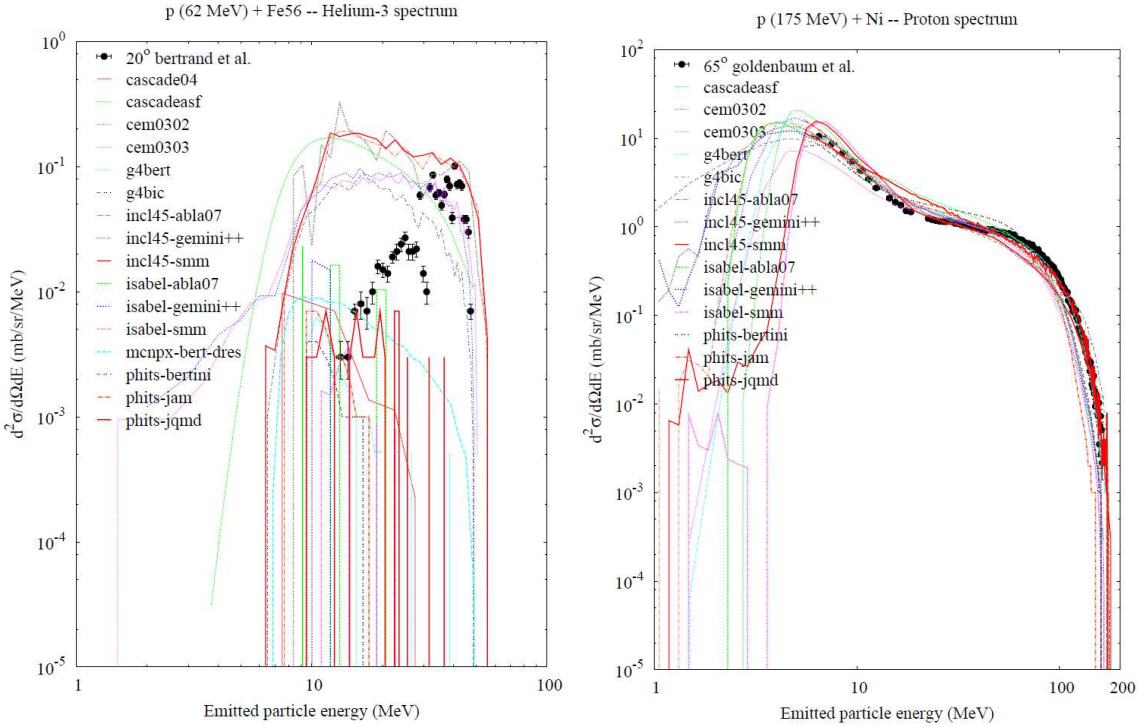


(a) worst case: He3 in 20 deg for 62 MeV protons on Fe-56

(b) best case: protons in 65 deg for 175 MeV protons on $Ni_{nat}$

Fig. 7: Extreme cases of predictions of double-differential cross sections.

Proton double-differential cross sections are predicted best; in the average over all experiments and all codes a rating of 2.4 was achieved followed by alpha, trition, deuteron and He3 cross sections with averaged ratings of 1.31, 1.18, 1.16 and 0.95, respectively. More than half of the codes have significant deficits in the prediction of higher-mass charged particle cross sections.

Viewing plots of double-differential cross sections make it obvious that these codes lack the emission of deuterons, tritons, He-3 and alphas at high energies in the INC phase and pre-equilibrium phase as seen for example in Fig. 8 for alpha emission at 35 degrees in reactions of 175 MeV protons on $Ni_{nat}$. The CEM03 codes, the INCL4.5 codes with the various de-excitation codes, and the CASCADE-ASF code are superior especially for emission of higher-mass charged particles because of employing coalescence models in the INC phase and/or pre-equilibrium models that provide higher-mass fragment emission channels.

Introducing an energy range of 0-20 MeV for the rating may have allowed testing charged particle emission in the evaporation phase, which is at present merged into a combined evaporation and pre-equilibrium group.

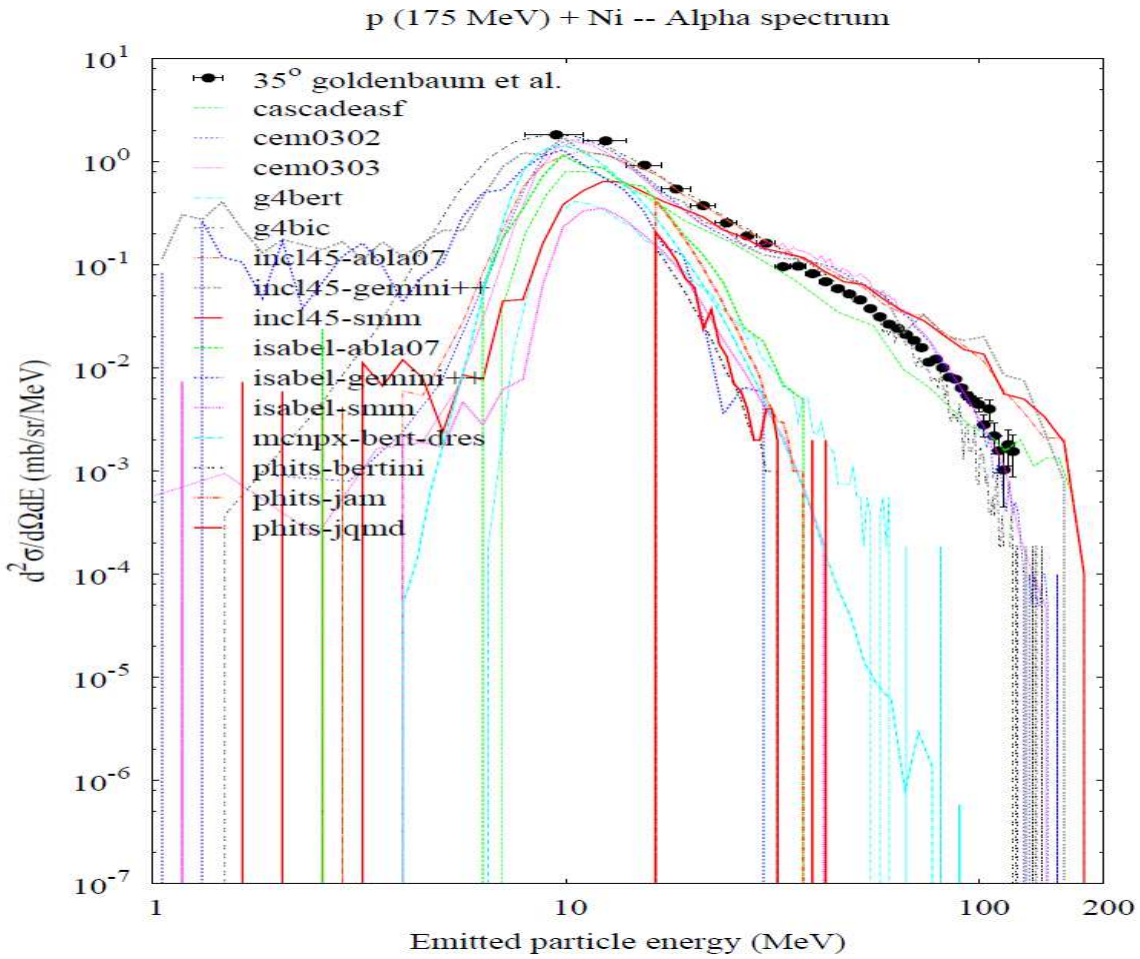


Fig. 8: Emission spectra of alphas at 35 deg in reactions of 175 MeV proton reactions on $Ni_{nat}$

Comparing Figs A1-3 with A5-6, a trend of degradation of the predictive power with increased incident energy is obvious for the CASCAD-ASF and the CEM03 codes, while the trend is reversed for INCL4.5 with the various de-excitation models.

**Benchmark Case Specific Findings and Remarks**

*62 MeV protons on Fe-56*

The resonance peaks at approximately 60 MeV for proton, deuteron emission are generally not well captured by the codes. GEANT-Bertini does quite well in decribing the peak for protons as shown in Fig. 9 but fails completely for the other charged particles. Generally the resonance peak is described too broad or just as a drop-off at high energies except for the PHITS codes, which exhibit a very narrow and too high spike following too pronounced a dip. Representative for this fact, the Bertrand data at 20 degrees are compared against the calculational results in Fig. 10.

Some of the experimental data seems questionable: a factor 2 step-down at energies around 9 MeV exists, and also the deuteron emission at 20 degrees shown in Fig. 7(a) seems undervalued below 40 MeV compared to the data at 37 degrees. All of the codes failed to predict this dataset. Consulting the bismuth and Pb-208 data for the same proton energy may give more insight.

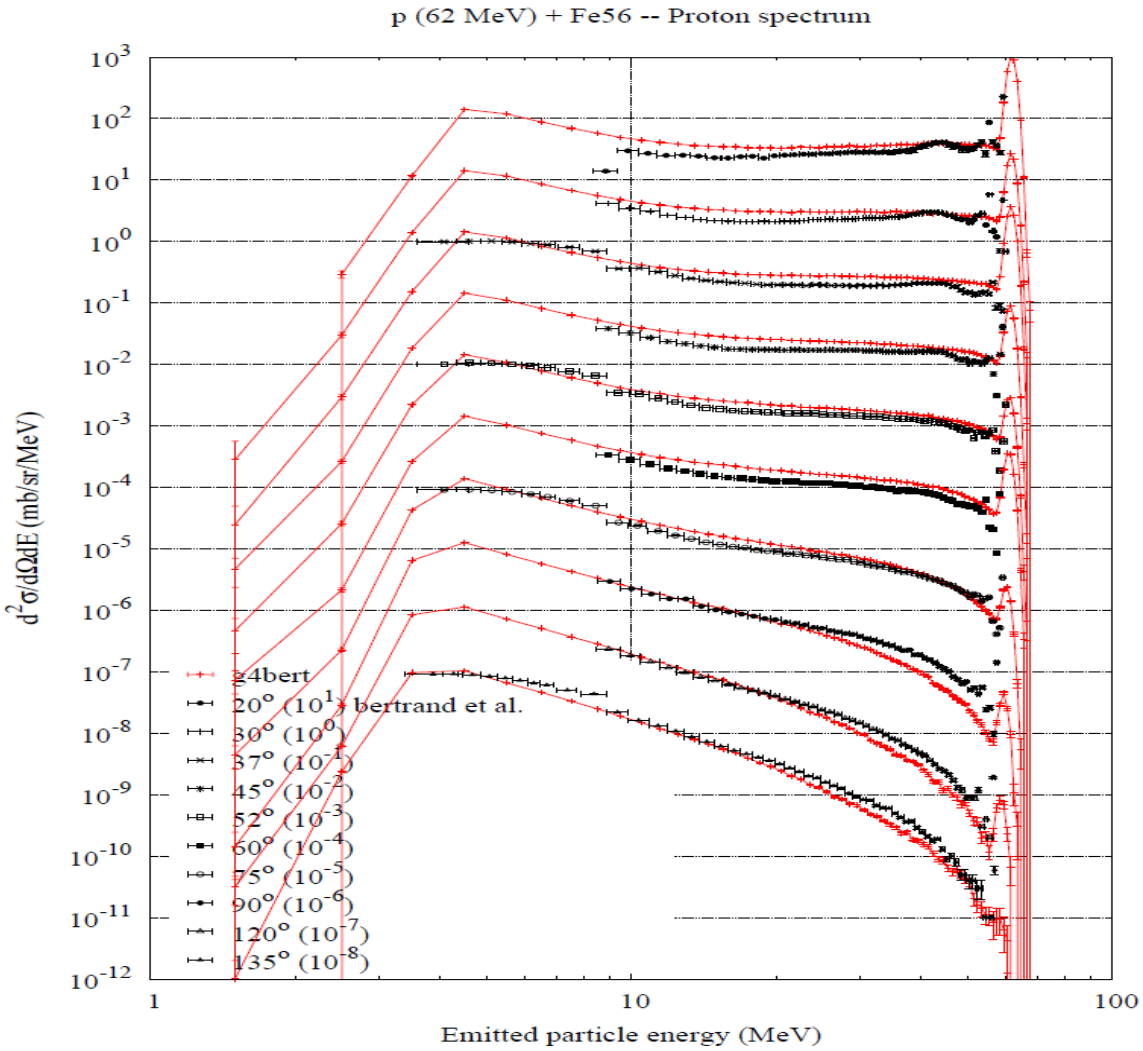


Fig. 9: Proton double-differential emission cross sections for 62 MeV protons on Fe-56 as predicted by GEANT4-Bertini.

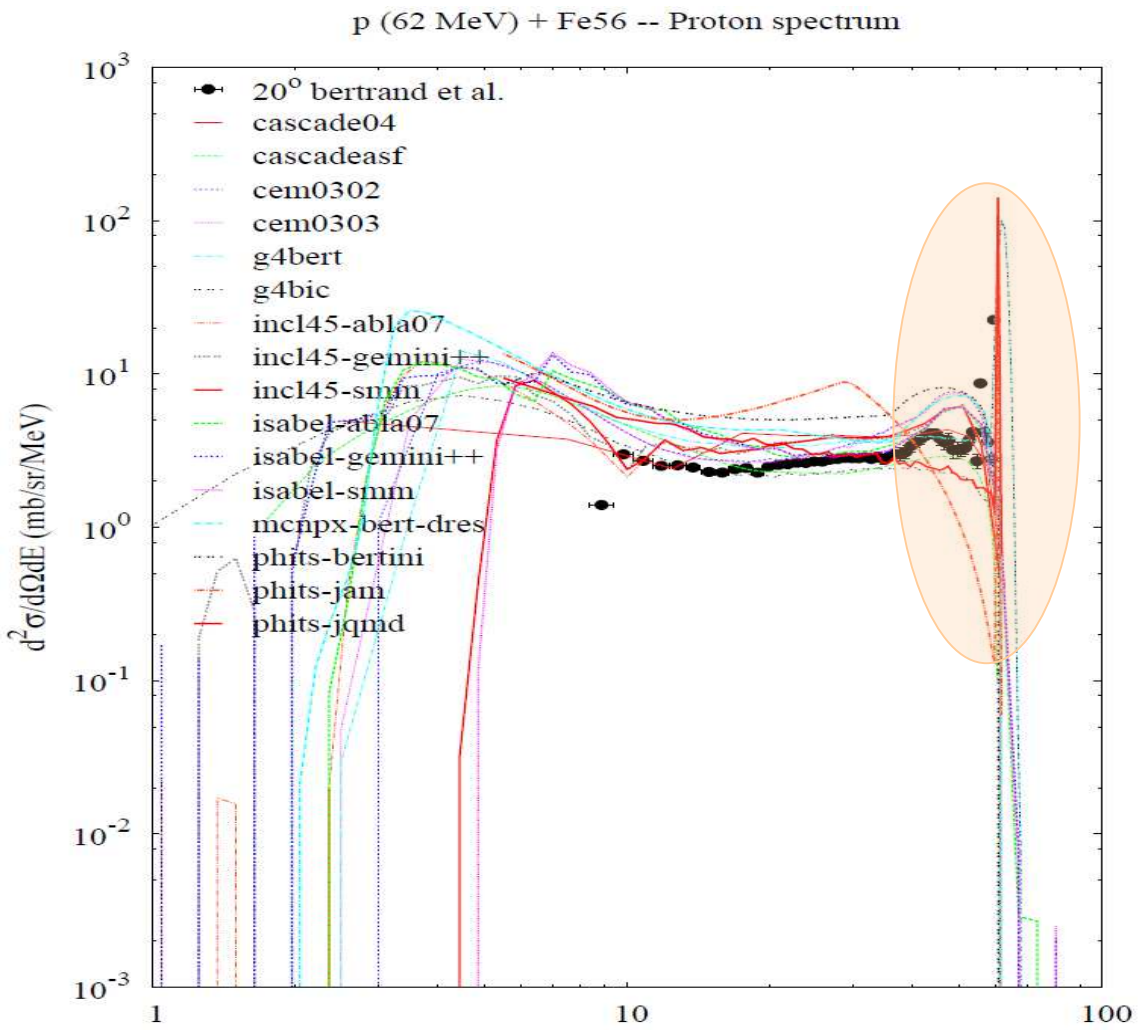


Fig. 10: Proton emission at 20 degrees for 62 MeV protons on Fe-56. Experimental double-differential cross sections from Bertrand et al are compared against calculational results.

*175 MeV protons on natural nickel*

The energy range of emitted particles differs with emission angle ranging from 2-8-20-150 MeV such that this benchmark set delivers puzzle pieces of emission spectra rather than a complete picture. This could be overcome for the proton spectra by supplementing the data set with the Frötsch data, which was not done at this stage of evaluation. A number of codes predicted these benchmark data fairly well (CASCAD-ASF, CEM03, INCL4.5) achieving ratings of 3 and better as documented in Fig. A.2.

For proton emission in the forward direction represented in Fig. 11, all codes with the exception of the PHITS-QMD code and with reservation the GEANT-BIC code, exhibit a bathtub type shape with a spectral depression at energies 20-80 MeV and developing a broad high-energy peak at forward emission, which is not supported by the experimental data.

For emission of the higher mass charged particles, the codes except INCL4.5 combinations underpredict the spectra at high energies. INCL4.5 on the other hand develops a pronounced high-energy peak at forward angles for deuterons, tritons and He-3, which the Goldenbaum data do not show.

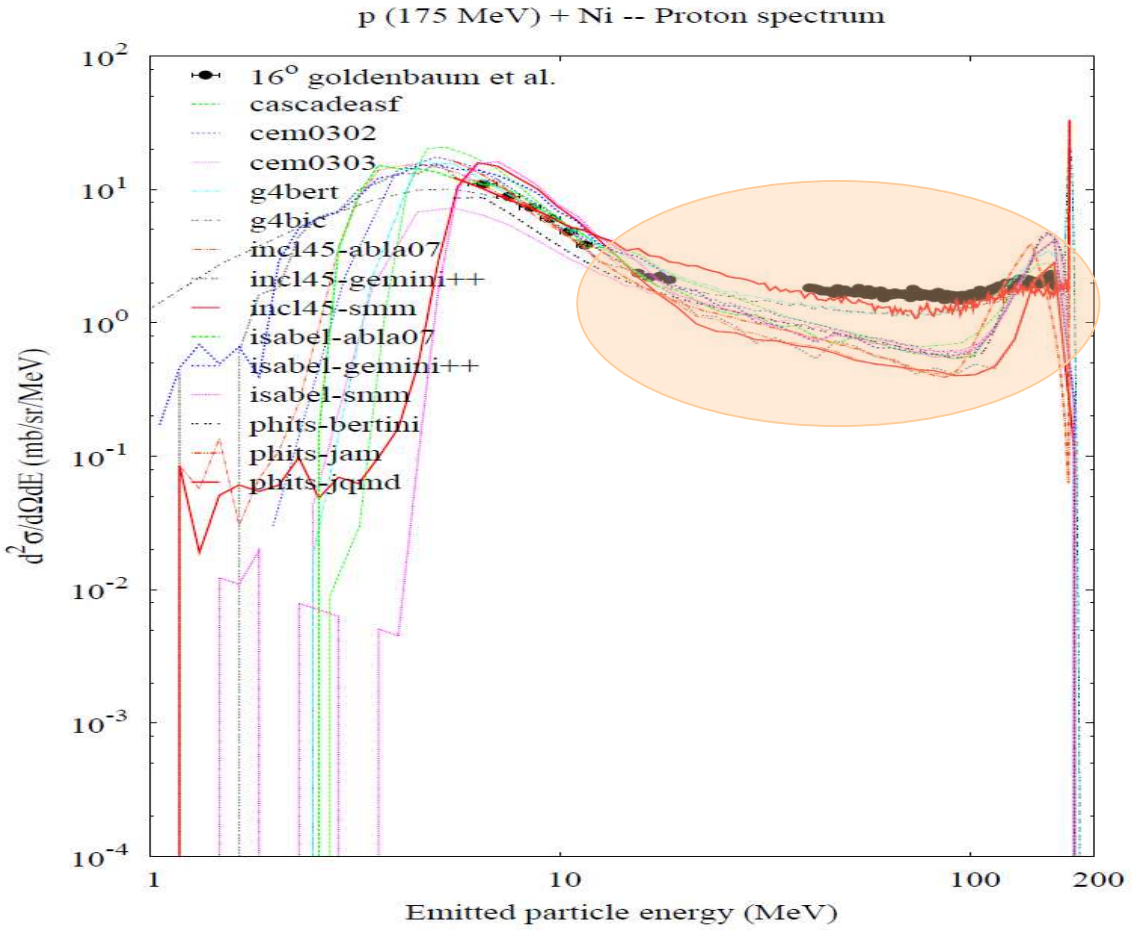


Fig. 11: Proton emission at 16 degrees for 175 MeV protons on $Ni_{nat}$. Experimental double-differential cross sections from Bertrand, et al, are compared against calculational results.

*542 MeV neutrons on bismuth*

This experiment was conducted by Franz et al with a continuous energy neutron beam peaking at high energies at 542 MeV but with neutron energies extending up to 590 MeV. By elaborate post-processing the double-differential production cross sections of protons, deuterons and tritons were extracted from time-of-flight data.

Almost all codes predict the proton double-differential cross section data very well. At 54 degrees, the most forward direction measured, the experimental data are underpredicted as highlighted in Fig. 12, which is very likely caused by performing the calculations at a discrete energy of 542 MeV neutron energy rather than the continuous energy nature of the experiment. At larger angles, the high-energy part of the spectrum

already has dropped significantly such that the continuous-energy nature of the incident beam does not play a role.

For deuteron and triton emission, the CEM03 versions are practically in line with the experimental data. CASCAD-ASF somewhat overpredicts for energies above 150 MeV, while the INCL4.5 combinations overpredict the experimental data over the whole energy range.

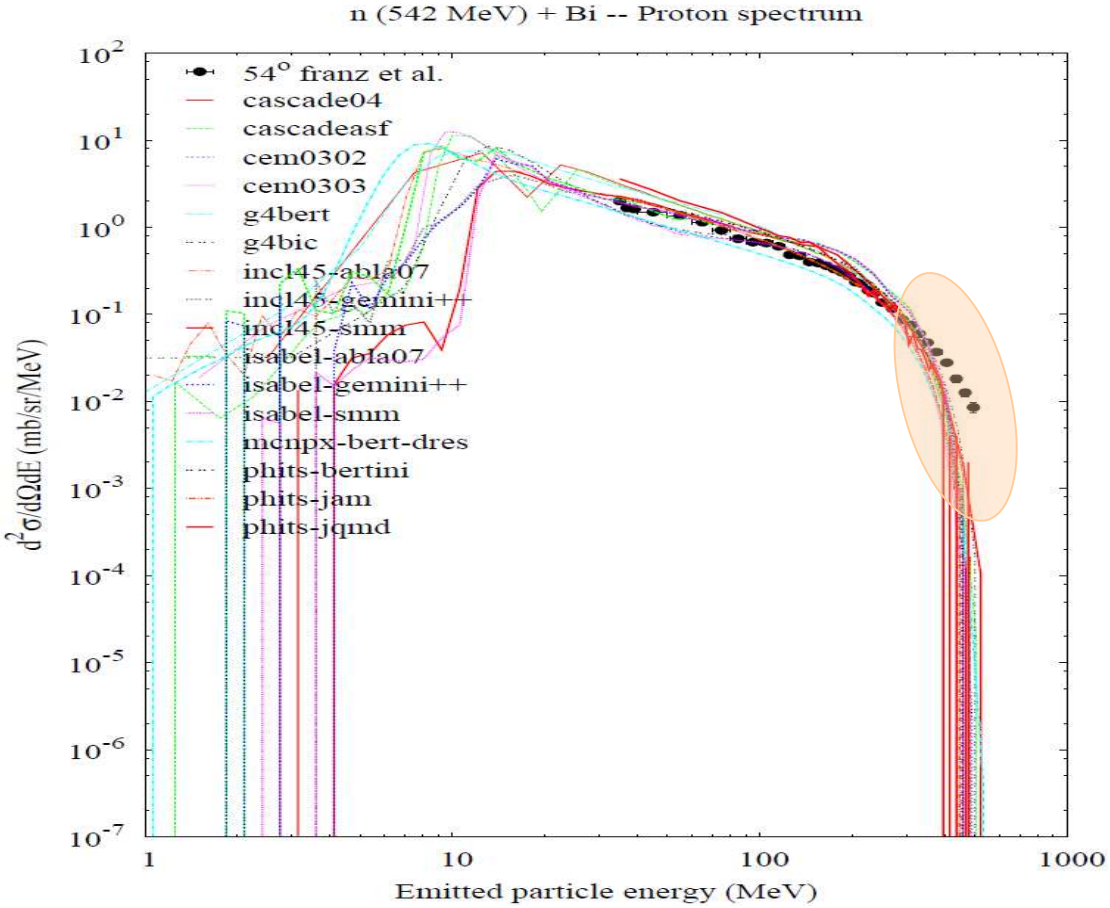


Fig. 12: Proton emission at 54 degrees for 542 MeV neutrons on $Ni_{nat}$. Experimental double-differential cross sections from Bertrand et al are compared against calculational results.

*800 MeV protons on Pb-208*

The experiment by McGill, et al, tests the proton emission in the forward direction at high energies showing a pronounced quasi-elastic peak at 5 degrees broadening and dropping in intensity with increasing angles.
Again we see confirmed in Fig. A.4 that proton emission is generally well described by all of the models. Very convincing are CASCADE04, CASCADE-ASF, INCL4.5, ISABEL, also GEANT4-BIC and all of the PHITS codes.

*1200 MeV protons on tantalum*

In contrast to the previously discussed data, the Herbach, et al, experiment investigates the emission at lower energies where the pre-equilibrium and evaporation processes come into play.
According to Fig. A.5, about one half of the codes predict proton production reasonably well. None of the codes is able to describe well the spectral slopes for energies of 10-100 MeV of the 30, 75 and 150 degree data as shown in Fig. 13 (the spike shown for PHITS-JQMD is caused by bad statistics). Also the evaporation peak is mostly overestimated.

For higher mass charged particle emission, INCL4.5 matches the experimental data with GEMINI and ABLA07 being superior to SMM. SMM seems to miss somewhat at the low-energy side of the evaporation peaks. The equilibrium de-excitation codes alone are not able to describe the emission data as seen in comparison of the ISABEL combinations as shown in the comparison of INCL4.5-ABLA07 and ISABEL-ABLA07 in Fig. 14. ISABEL uses the same de-excitation codes as INCL4.5 but does not adequately predict the "pre-equilibrium" phase – it does not employ a pre-equilibrium model and does not offer higher-mass charged particle emission in the INC phase. This issue is shared with a number of other codes.

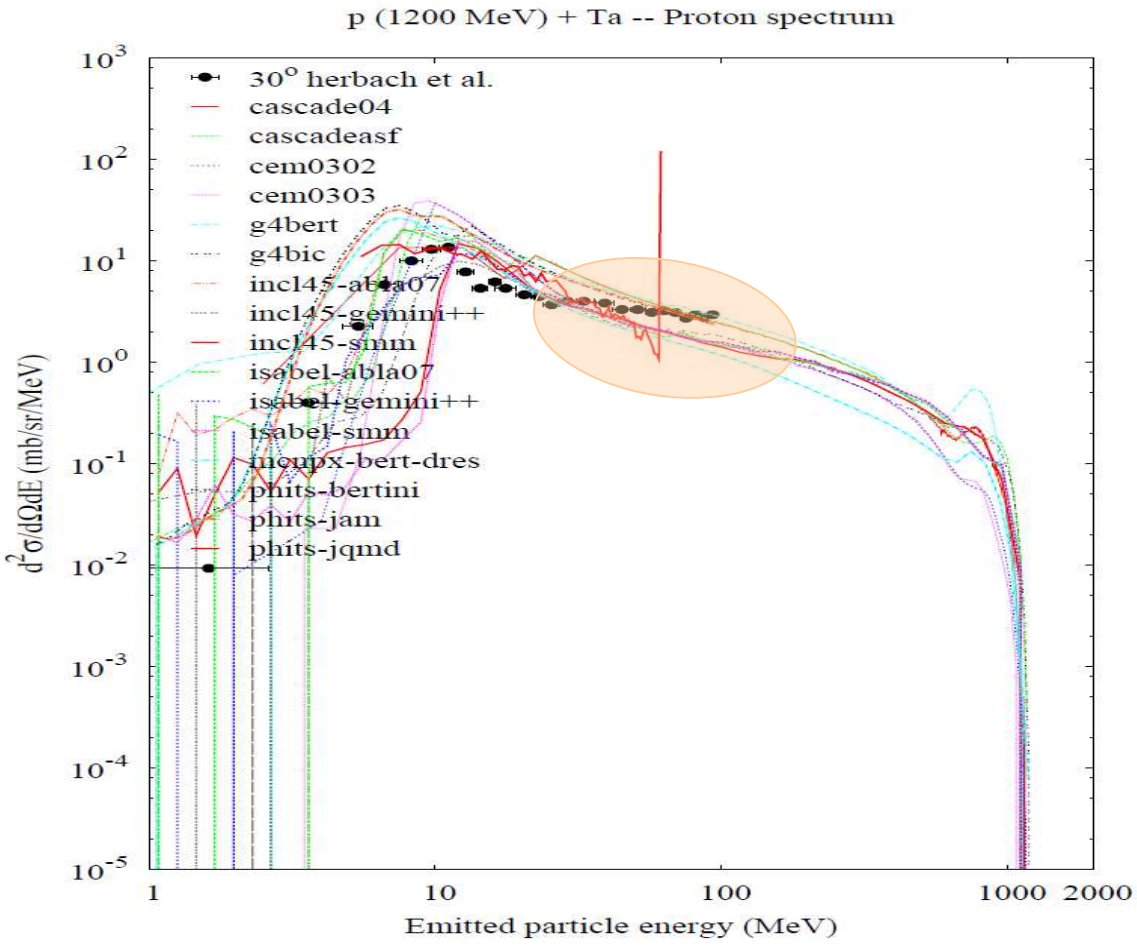

Fig. 13: Proton emission at 30 degrees for 1200 MeV protons on tantalum. Experimental double-differential cross sections from Herbach, et al, are compared against calculational results.

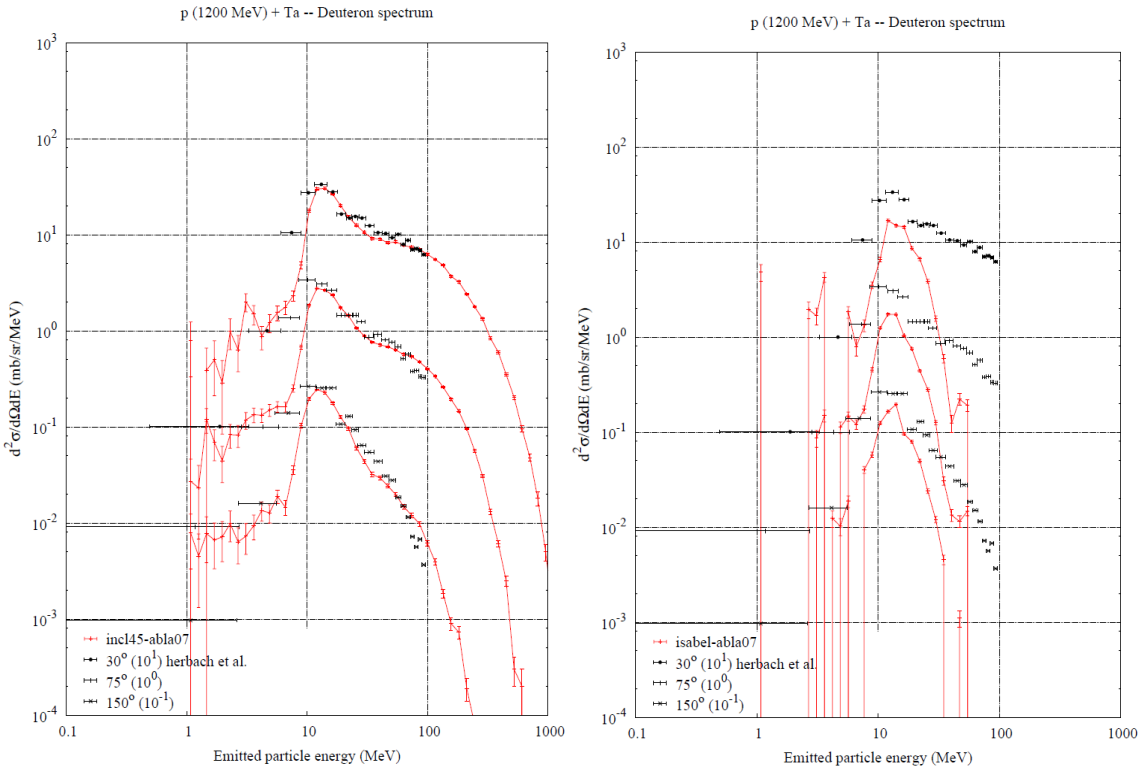


Fig. 14: Comparison calculational results of Deuteron emission from INCL4.5-ABLA07 and ISABEL-ABLA07 against data measured by Herbach, et al, for 1200 MeV protons on tantalum.

*2500 MeV protons on gold*

The Bubak, el al, data looking at charged particle emission for 2500 MeV protons on gold are similar in character as the Herbach data discussed in the previous subsection. The studied emission energies are covered by equilibrium and pre-equilibrium emission effects.

None of the codes is able to predict the spectral shape at energies 20-150 MeV where the spectrum flattens out and distinguishes itself from the evaporation peak. This separation is more pronounced in forward directions. The findings of code predictions are similar to that for the Herbach data.

**Conclusion**

With adding light charged particle double-differential cross sections, the International Spallation Models Benchmark Effort extended the testing terrain to new dimensions. The comparison gives the users a measure of the predictive power of the codes, and the code

developers useful information about strengths and weaknesses of their codes and possible paths of improvements researching the underlying physics of their competitors.

Already this preliminary evaluation gives us the clear picture that the light charged particle emission has a lot of room for improvement to raise it to the level of the prediction of neutron production.

Major work needs to be completed in two areas:

- Including complex light charged particle emission already in the first phase of the spallation reaction is crucial to describe the particle spectra. A number of contributors lack this part of physics and therefore are not able to compete in describing higher-mass double-differential cross sections. It may even be interesting to extend the listing of considered particles to lithium and beryllium isotopes as experimental data exist.

- The description of proton emission has deficits in the forward direction. For emission energies between 20 and 150 MeV for medium mass targets and low projectile energies, the experiments show plateauing but the codes exhibit bathtub-like depressions. For the high-mass targets with 800 MeV incident protons, the spectral shapes in the forward direction seem fine at high energies with lacking data being for the equilibrium and pre-equilibrium energies. However, systematic problems seem to exist for higher projectile energies and high-mass targets. Again the spectral shape extends in a plateau from the equilibrium emission peak to higher energies. None of the codes was able to describe this transition. Unfortunately, the experimental data do not extend beyond emission energies of 100 MeV in the chosen benchmark data, so no insight can be gained about the spectra at higher energies. It may be interesting to supplement the benchmark data by medium mass target reactions at high projectile energies as they exist.

**References**


Blann, M., Gruppelaar, H., Nagel, P., Rodens, J.; International Code Comparison for Intermediate Energy Nuclear Data, NEA/OECD, NSC/DOC(94)-2, Paris 1993.
J. Franz et al., Nucl. Phys. A 510 (1990) 774
A. Cowley et al., Phys. Rev. C 54 (1996) 778
F.E. Bertrand and R.W. Pelle, Phys. Rev. C 8 (1973) 1045
F. Goldenbaum et al., (unpublished)
S.V. Förtsch et al., Phys. Rev. C 43 (1991) 691
C.-M. Herbach et al., Nucl. Phys. A 765 (2006) 426
A. Cowley et al., Phys. Rev. C 54 (1996) 778
A. Budzanowski et al., Phys. Rev. C 78 (2008) 024603
A. Letourneau et al., Nucl. Phys. A 712 (2002) 133
A. Bubak et al., Phys. Rev. C 76 (2007) 014618
A. Guertin et al., Eur. Phys. J. A 23 (2005) 49

R. Chrien et al., Phys. Rev. C 21 (1980) 1014
J.A. McGill et al., Phys. Rev. C 29 (1984) 204
F.E. Bertrand and R.W. Pelle, Phys. Rev. C 8 (1973) 1045

**Appendix:**

**Summary Plots of Code Ratings by Experimental Datasets**

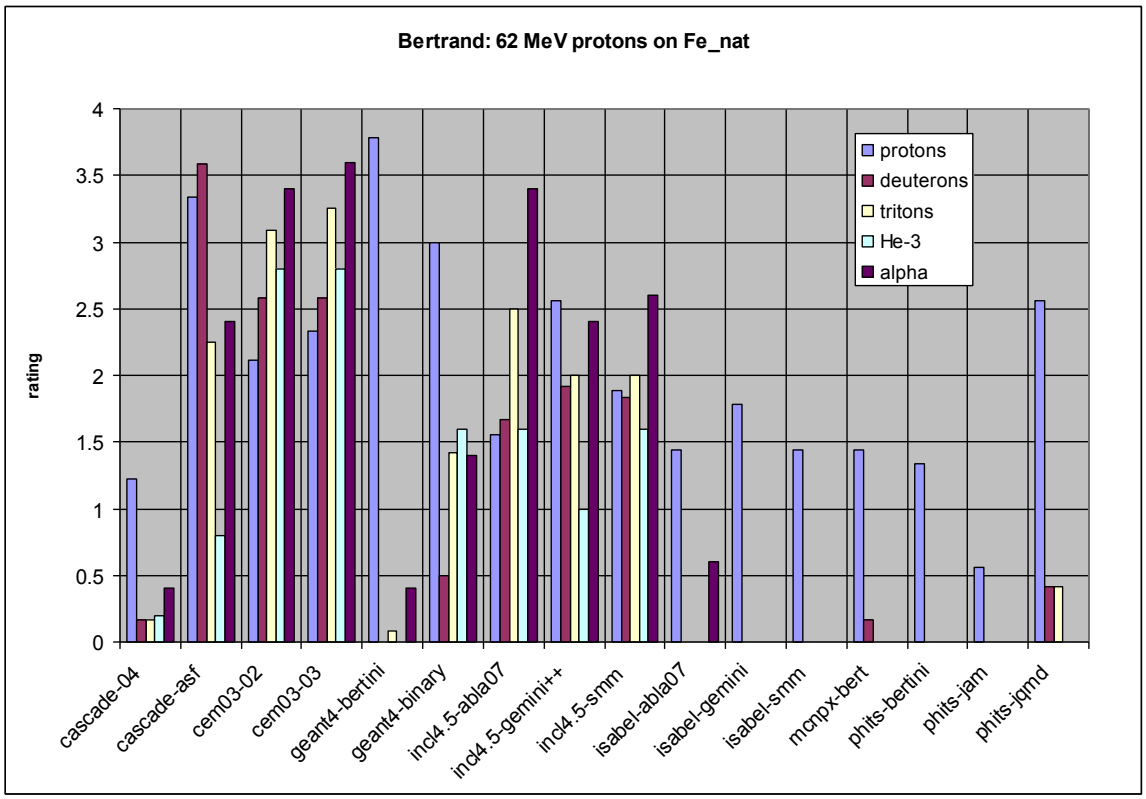


Fig. A.1: Code evaluation for the data set of 62 MeV protons on $Fe_{nat}$ by Bertrand et al.

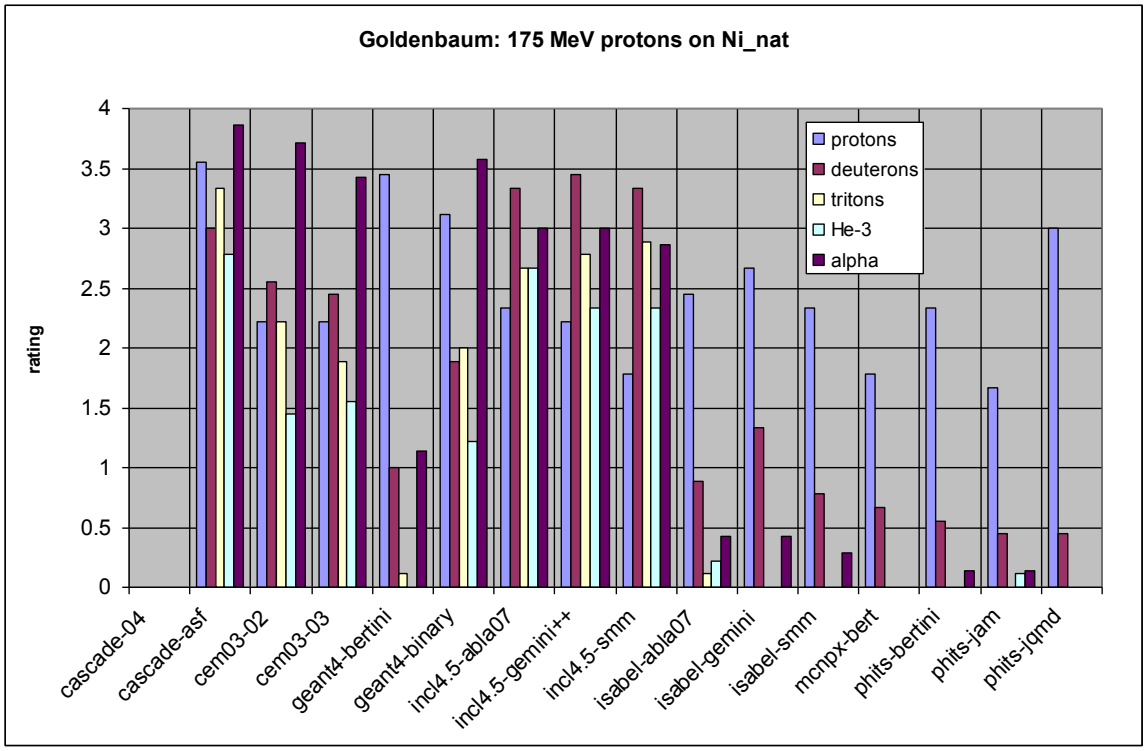


Fig. A.2: Code evaluation for the data set of 175 MeV protons on $Ni_{nat}$ by Goldenbaum et al.

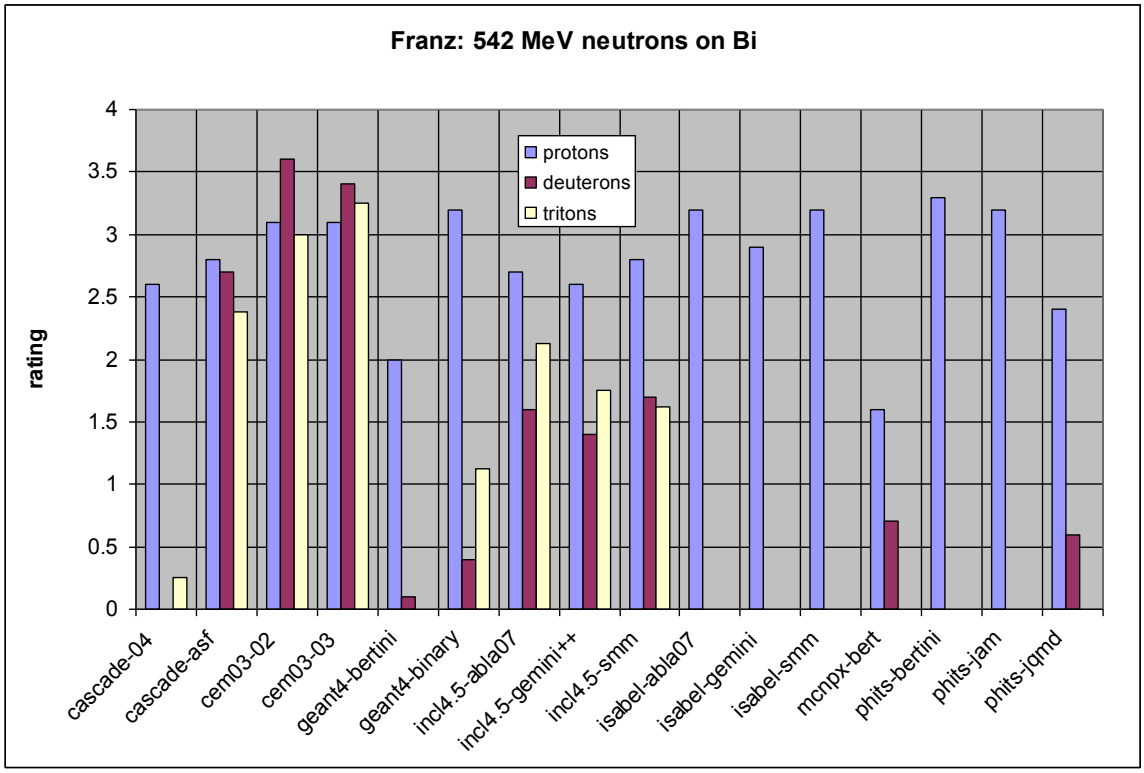


Fig. A.3: Code evaluation for the data set of 542 MeV neutrons on Bi by Franz et al.

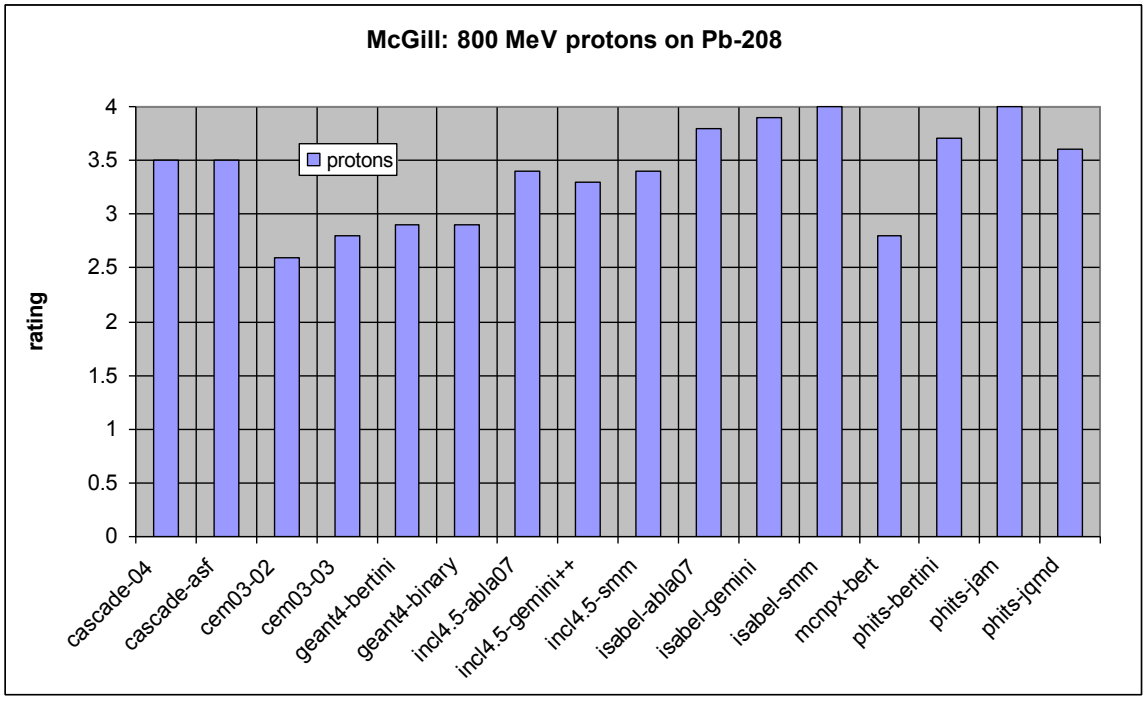


Fig. A.4: Code evaluation for the data set of 800 MeV protons on Pb-208 by McGill et al.

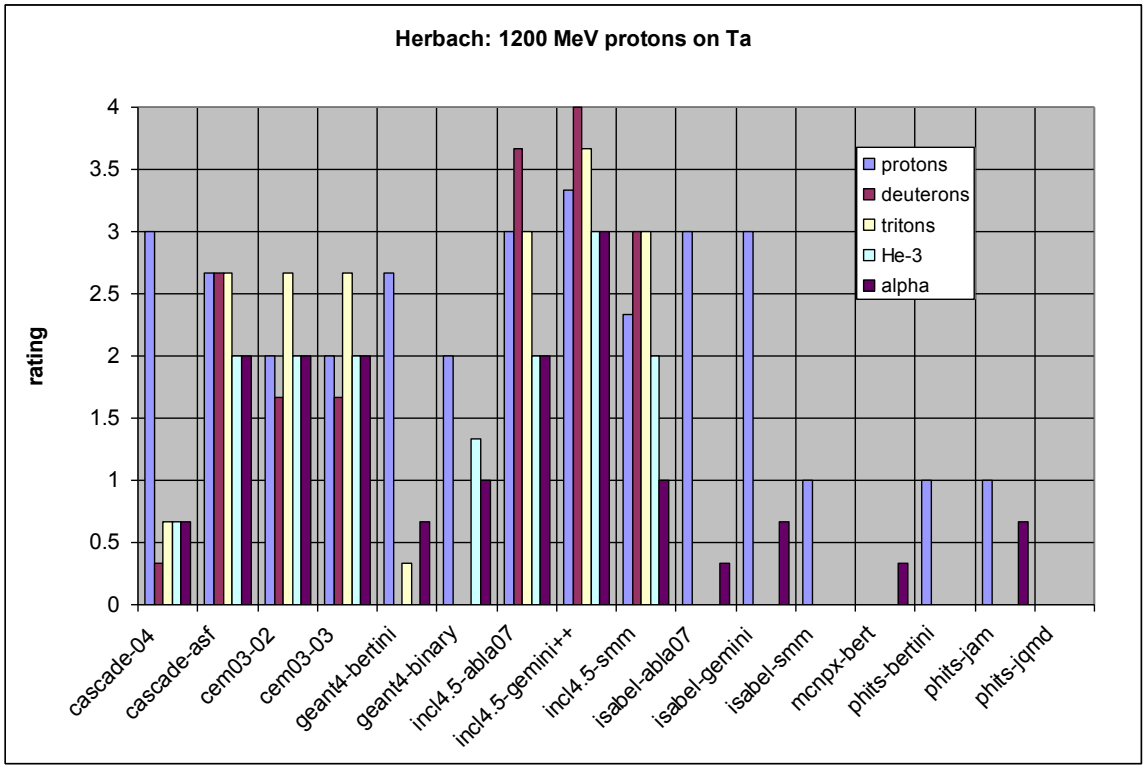


Fig. A.5: Code evaluation for the data set of 1200 MeV protons on Ta by Herbach et al.

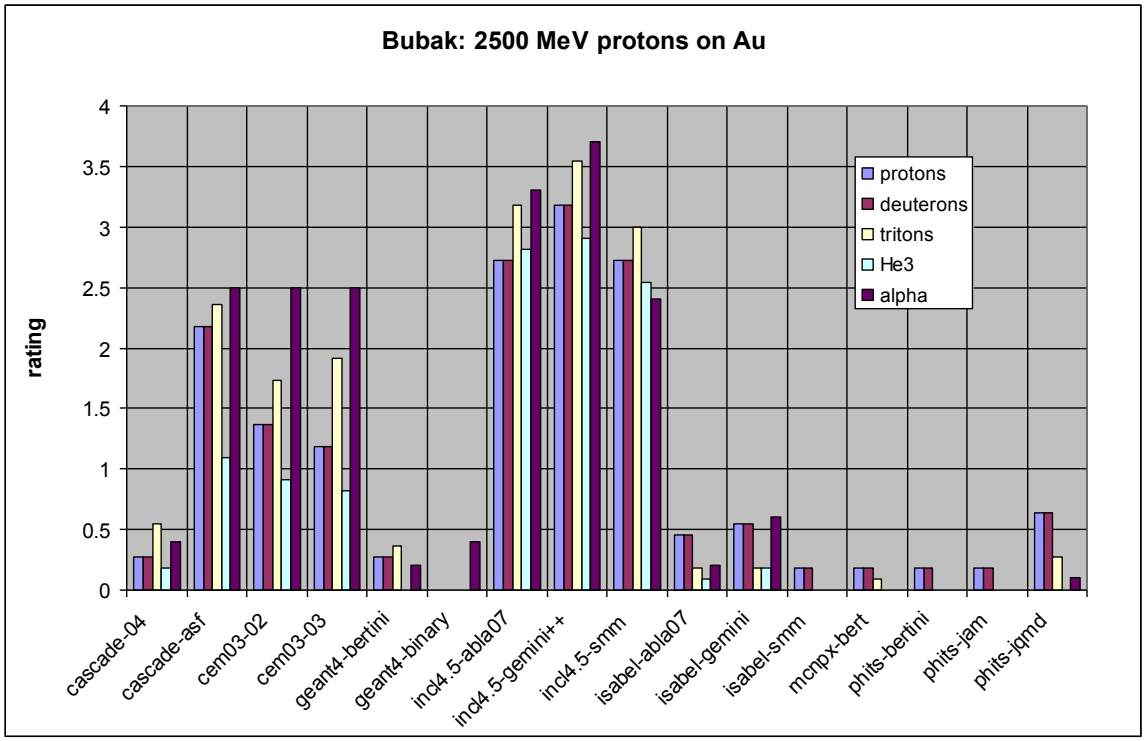


Fig. A.6: Code evaluation for the data set of 2500 MeV protons on Au by Bubak et al.